

Spin Excitation in *d*-wave Superconductors : A Comprehensive Study Based On The Fermi Liquid Picture

Khee-Kyun Voo, Hong-Yi Chen, and W. C. Wu

Department of Physics, National Taiwan Normal University, Taipei 11650, Taiwan, R.O.C.

(December 2, 2024)

A detailed study of the Inelastic Neutron Scattering (INS) spectra of the high- T_c cuprates based on the Fermi liquid (FL) picture is given. We emphasize on the issue of transformation between the commensurate and incommensurate (IC) excitation driven by frequency or *temperature*, and this is intended to be compared with the Stripe picture of the system. For $\text{La}_{2-x}\text{Sr}_x\text{CuO}_4$ (LSCO), the condition $\Delta(0)/v_F \ll \pi$ (where we have set the lattice constant to 1) consistently describes the always existing IC peaks in the superconducting (SC) and normal state, and static location at temperature or frequency change. For $\text{YBa}_2\text{Cu}_3\text{O}_{6+x}$ (YBCO), an appreciable nonzero $\Delta(0)/v_F$ and proximity of the van Hove singularity (vHS) at $\overline{M} = (0, \pi)$ to the Fermi level consistently describe the frequency- and temperature-driven shifting IC peaks in the SC state, the vanishing of the IC peak in the normal state, and the existence of the commensurate peak in the SC state. We address the conditional peak shifting behavior to a refined consideration on the nesting effect which is previously overlooked. The $\Delta(0)/v_F \ll \pi$ limit is also found to suppress the possibility of Random-Phase-Approximation (RPA) commensurate resonance at $\omega/\Delta < 2$. As a result, the very recently reported contrasting behaviors of YBCO when compared to LSCO, on $\text{YBa}_2\text{Cu}_3\text{O}_{6.7}$ by Arai *et al.* [1] and $\text{YBa}_2\text{Cu}_3\text{O}_{6.85}$ by Bourges *et al.* [2] can be reasonably reconciled in a FL picture. We also point out that the one-dimensional-like data by Mook *et al.* [3] on a detwinned and more underdoped sample $\text{YBa}_2\text{Cu}_3\text{O}_{6.6}$ could be due to a gap anisotropy effect discussed by Rendell and Carbotte [4], and we proceed to suggest a way of clarifying it.

I. INTRODUCTION

The aim of this paper is twofold. The first is to give a comprehensive study of the major properties of the BCS spin susceptibility. The second, base on that we account for the intriguing present situation that the INS data of YBCO shows contrasting behaviors when compared to LSCO. The one-dimensional nature of Mook *et al.*'s data is also discussed.

Magnetic fluctuation in the high- T_c cuprates has been long believed to be very intimately related to its superconductivity mechanism. Therefore various kinds of magnetic measurements such as Nuclear Magnetic Resonance (NMR), Nuclear Quadrupole Resonance (NQR), and INS have been carried out on the system, and aimed for clarifying the connection between the two. Among those measurements, INS experiments is the one which distinguishes itself from others by its capability to measure the fluctuation locally in momentum and frequency space and hence making itself an indispensable and important tool. Especially recently it provides a great deal of new observations, which has yet reached a consensus.

Essentially there are two dominant features of the observed INS spectra, the existence of commensurate peak at $\mathbf{Q}_{AF} \equiv (\pi, \pi)$, and IC peak at $\mathbf{Q}_\delta \equiv (\pi, \pi \pm \delta)$ and $(\pi \pm \delta, \pi)$. The spectra in LSCO [5–7] is always IC and have a fixed incommensurability independent of ω and T but increases with hole-doping. On the other hand, YBCO [2,1,8] and $\text{Bi}_2\text{Sr}_2\text{CaCu}_2\text{O}_{8+x}$ (BSCCO) [9,10] compounds exhibit both commensurate and IC peaks.

Very recently a comprehensive INS data on YBCO is obtained [2,1]. In the low temperature SC state, it shows a commensurate peak at a particular frequency $\omega_o(T = 0)$, and departing from ω_o (either go below or above ω_o) the peak is split up into IC and the incommensurability is continuously increased. The IC peak is found only above some threshold frequency. In the normal state, the excitation is always a broad commensurate or weakly IC structure. The incommensurability of the low frequency IC structure at low temperature is continuously closed up to commensurate by rising temperature to T_c . Such behavior is seen in an underdoped [1] and nearly optimally doped YBCO [2] (while YBCO data on a broad doping range are not available). These behaviors are in strong contrast to LSCO, and therefore raises an important question as whether the INS spectra in YBCO and LSCO are of the same origin.

There are also reports of the observation of the commensurate resonance in the pseudo-gap phase of underdoped YBCO, at the same frequency as in the SC phase but that remains controversial [11]. At all doping levels, its resonance nature is only well-established in the SC phase.

Perhaps the most straightforward and simplest interpretation of the IC peak is the Fermi surface (FS) nesting effect (see e.g. Ref. [12–16] and references therein). Many of the theoretical approaches assume the system is spatially homogeneous and ultimately end up at a FS, could be it a FS of conventional electrons or a FS of some exotic fermion such as the spinon. The spin excitation is consti-

tuted by those low energy excitations nearby the surface. Such scenarios are capable of producing frequency-shifted IC peaks [12–14], and furthermore, the commensurate peak is easily derived from it either at the bare or RPA level.

The Stripe ordering picture [17] is an alternative which predicts static IC peaks in spin and charge excitations that have incommensurability directly proportional to, and only depend on doping. In this picture the system is segregated into one-dimensional hole-rich stripes in which the holes can freely move, and electron-rich stripes in which electrons are ordered antiferromagnetically. The electron filling determines the length scales and thus the incommensurability. It is believed that the static stripe at the 1/8-doping [18], and the 2-to-1-coupled charge and spin excitations [19] are observed. That has boost a lot of works on the “dynamic” stripe which also aimed at the connection with the superconductivity mechanism. A plain Stripe model predicts no commensurate peak.

Therefore the Stripe picture seems to work well in LSCO, while the FL picture works well in YBCO. Here we argue that the discrepancies could be reconciled if the problem is considered more carefully. The frequency and temperature driven peak shifting present in YBCO but not in LSCO can be accounted for by a flatter electronic dispersion near FS such that the excitation can scattered farther from it, while electronic dispersion of LSCO near FS is far more steep. A refined consideration of the nesting effect, which we have termed the *dynamic local nesting* effect is important when the condition $\Delta/v_F \ll \pi$ is violated. In the regime of having shifting IC peak in SC state, the IC peak is necessarily vanishes in the normal state. The commensurate resonance in the SC state of YBCO and BSCCO is addressed as a consequence of the experimentally observed closeness of the vHS at \bar{M} to the Fermi level [20–24]. The effect of the band singularity has been shown in many cases to be significant, such as providing the vanishing isotope effect, transport anomalies, high SC transition temperature, and so on. In short, we have argued that the apparently contradictory INS data can have a common basis in the FL regime.

We should also mention the data of Mook *et al.* [3] on a detwinned and more underdoped YBCO, $\text{YBa}_2\text{Cu}_3\text{O}_{6.6}$. The one-dimensional nature of the data where the IC peaks are found only along one of the crystal axis, is claimed by the authors as a strong evidence of stripe’s existence. Nevertheless we point out in Sec. VII that such behaviors can be due to an anisotropy effect in the FL picture. The effect is prominent in the frequency regime where the data in Ref. [3] was taken.

This study is also important in the aspect that it provides a comprehensive and detailed survey of the major consequences from the FL picture, and thus acts as a reference to see how much of the experimentally observed behaviors really are deviating from the FL. Comparison with experiments are made where possible. Some of the materials in this paper already have appeared in the ex-

isting literature, we include them here to facilitate discussion and refer the reader to the literature for more details.

Our discussion will be focused on the evolution of the peak intensity, width, and location in the parameter space of ω and T . We organize this paper into sections and a brief summary of the findings of each sections or subsections is given at their ends where it is necessary. The first several sections are focused on the IC excitation without any band singularity effect, and the commensurate resonance is studied after the general discussion on the RPA susceptibility. Sec. II gives the formalism. Sec. III gives the bare spectra in SC state, normal state, and at the transition. Cases like varying the ratio of SC gap to Fermi velocity Δ/v_F are studied. Sec. IV discusses the underlying machinery of the formation and behaviors of the IC peaks. Sec. V studies the effect of inclusion of the Hubbard repulsion or AF interaction into the system via the RPA. An appropriate description of LSCO is discussed. Sec. VI is devoted to the relation between the commensurate excitation and \bar{M} -point vHS. An appropriate description of YBCO is then discussed. Sec. VII is a discussion on the anisotropy effect and the one-dimensional nature in INS spectrum. Finally, Sec. VIII gives our discussion of the results and conclusions.

II. FORMALISM

What we need in a FL description of the INS spectrum is the existence of a well-defined FS and the dispersion nearby. All low energy processes are constituted by the excitation at the vicinity of the surface.

The INS spectrum is proportional to $\text{Im}\chi(\mathbf{q}, \omega)$ besides some Bose-Einstein distribution factor due to the bosonic character of the excitation. $\chi(\mathbf{q}, \omega)$ is the spin susceptibility. The BCS bare spin susceptibility is given below and followed by the RPA-corrected susceptibility.

The BCS bare spin susceptibility in a one-layer SC system (the susceptibility in normal system could be obtained by letting $\Delta \rightarrow 0$) is

$$\begin{aligned} \chi_o(\mathbf{q}, \omega) = & -\frac{1}{4} \sum_{\mathbf{k}} \left[\left[1 - \frac{\xi_{\mathbf{k}}\xi_{\mathbf{k}+\mathbf{q}} + \Delta_{\mathbf{k}}\Delta_{\mathbf{k}+\mathbf{q}}}{E_{\mathbf{k}}E_{\mathbf{k}+\mathbf{q}}} \right] \right. \\ & \times \left[\frac{1 - f(E_{\mathbf{k}}) - f(E_{\mathbf{k}+\mathbf{q}})}{\omega - E_{\mathbf{k}} - E_{\mathbf{k}+\mathbf{q}} + i\Gamma} - \frac{1 - f(E_{\mathbf{k}}) - f(E_{\mathbf{k}+\mathbf{q}})}{\omega + E_{\mathbf{k}} + E_{\mathbf{k}+\mathbf{q}} + i\Gamma} \right] \\ & - \left[1 + \frac{\xi_{\mathbf{k}}\xi_{\mathbf{k}+\mathbf{q}} + \Delta_{\mathbf{k}}\Delta_{\mathbf{k}+\mathbf{q}}}{E_{\mathbf{k}}E_{\mathbf{k}+\mathbf{q}}} \right] \\ & \left. \times \left[\frac{f(E_{\mathbf{k}}) - f(E_{\mathbf{k}+\mathbf{q}})}{\omega - E_{\mathbf{k}} + E_{\mathbf{k}+\mathbf{q}} + i\Gamma} - \frac{f(E_{\mathbf{k}}) - f(E_{\mathbf{k}+\mathbf{q}})}{\omega + E_{\mathbf{k}} - E_{\mathbf{k}+\mathbf{q}} + i\Gamma} \right] \right], \quad (1) \end{aligned}$$

where \mathbf{q} and ω are respectively the momentum and energy transfers. $f(E_{\mathbf{k}})$ is the Fermi function and $E_{\mathbf{k}} = (\xi_{\mathbf{k}}^2 + \Delta_{\mathbf{k}}^2)^{1/2}$ is the quasiparticle spectrum with $\xi_{\mathbf{k}}$ and

$\Delta_{\mathbf{k}}$ the band dispersion and SC gap respectively. Henceforth we will write $\chi'_o \equiv \text{Re}\chi_o$, $\chi''_o \equiv \text{Im}\chi_o$, and likewise for χ in Eq. (3).

We use a two-dimensional tight-binding electronic dispersion

$$\xi_{\mathbf{k}} = -2t(\cos k_x + \cos k_y) - 4t' \cos k_x \cos k_y - \mu, \quad (2)$$

where t and t' are the nearest-neighbor (NN) and next-nearest-neighbor (NNN) hopping respectively. μ is the chemical potential that depends on doping. In this paper only the $d_{x^2-y^2}$ -gap is treated (except in Sec. VII) since it is meant to describe the high- T_c cuprates. It is taken as $\Delta_{\mathbf{k}} = \Delta(T)(\cos k_x - \cos k_y)/2$. The width Γ/t in numerical integration is taken within $0.002 \sim 0.008$ with slicing 2000×2000 or 4000×4000 .

Equation (1) describes two kinds of excitation, the pair-breaking excitation that excites two particles from the SC condensate and costs energy $E_{\mathbf{k}} + E_{\mathbf{k}+\mathbf{q}}$, and the thermal one-particle excitation that excites a particle from $\mathbf{k} + \mathbf{q}$ to \mathbf{k} which costs energy $E_{\mathbf{k}} - E_{\mathbf{k}+\mathbf{q}}$. The two-particle excitation vanishes in the normal state while the one-particle excitation vanishes at zero temperature SC state.

We have chosen a simple electronic dispersion with only the NN and NNN hopping considered. It is adopted for the sake of a simpler discussion and it is not expected that any qualitative different results will be obtained if a more complicated dispersion is adopted. Those properties of the system we want to model include the curvature of the FS near the SC gap nodes, and the steepness of the dispersion at FS. The Luttinger theorem (which states that the ratio of the volume within the FS to the total volume in the phase space is equal to the carrier density) will not be purposely preserved since it only complicates the matter.

The most important correction to the susceptibility should be the existence of Coulomb or AF correlations between the quasiparticles. Such correlations are believed to exist as a residual interaction between the renormalized particles, and they are conventionally treated by mean field decoupling as a nontrivial step beyond bare theories. Then the susceptibility is written into a simple RPA form as

$$\chi(\mathbf{q}, \omega) = \frac{\chi_o(\mathbf{k}, \omega)}{1 - V_{\mathbf{q}}\chi_o(\mathbf{k}, \omega)}, \quad (3)$$

where $V_{\mathbf{q}}$ can be the vertex of Hubbard repulsion U or AF interaction

$$J_{\mathbf{q}} = -\frac{|J|}{2}(\cos q_x + \cos q_y). \quad (4)$$

$J_{\mathbf{q}}$ is different from U essentially at being positive near \mathbf{Q}_{AF} and changing its sign to negative near $(0, 0)$. The RPA-type correction is important because it is perhaps the only way to treat correlation effect analytically.

III. EXCITATION AT BARE LEVEL — SURVEY OF BASIC PROPERTIES

We have given in this section a survey of the major properties of the bare excitation spectrum, and their discussion will be given in Sec. IV. Dispersions considered here are free from any singularity effect and an important band singularity effect will be studied in Sec. VI.

A. Superconducting State

The SC state is described by $\Delta(T) \neq 0$, which enters the quasiparticle spectrum as an excitation gap and results in a SC coherence factor.

It is important to note that the parameter Δ/t in our context is a phenomenological description of Δ/v_F , where v_F is the dispersion gradient at the FS. It is a measure of the portion of the phase space involved in low energy measurements, and manifested as the momentum width of the IC peaks in bare spectra. We mean no direct relevance to the overall bandwidth, and moreover, the dispersion near the Fermi surface could be strongly renormalized by factors such as particle-particle correlations and so on to deviate from the simple tight-binding band. A greater value of our Δ/t simply means a larger Δ or a flatter dispersion at the Fermi level.

Figure 1 shows the frequency-evolution of the spectra for two typical cases of Δ/t . We have ignored the well-discussed quasielastic node-to-node IC peaks [25] at the locations $(\pi + \delta_o, \pi \pm \delta_o)$ and $(\pi - \delta_o, \pi \pm \delta_o)$ and focused on the nesting IC peaks at the 45-degree rotated locations $(\pi, \pi \pm \delta)$ and $(\pi \pm \delta, \pi)$. As ω is increased, the intensity and widths of the peaks are increased, and spectrum at \mathbf{Q}_{AF} is filled in at some frequency near 2Δ which depends only on band geometry and independent of Δ/t . When Δ/t is large, the fill-in is stepwise due to a push in of a step-like feature. This sharper increase of $\chi''_o(\mathbf{Q}_{AF}, \omega)$ has an important relation to the resonance at \mathbf{Q}_{AF} and will be discussed in Sec. VI. The nesting IC peaks are seen to be sharpest at some intermediate frequencies before the filling in.

The larger Δ/t calculation [see Fig. 1(b)] shows broader and biased peaks that clump into \mathbf{Q}_{AF} with increasing frequency. This behavior is more pronounced when the RPA-correction is considered [see Secs. V and VI]. Such converging of the IC peak cluster was observed experimentally in YBCO and discussed by us [14] and other groups [26,13,12]. Here we proceed to give the full explanation in Sec. IV. The IC structure is destroyed after the peaks clump in at $\omega/\Delta \lesssim 2$, this is in contrast to the well-preserved static peaks in the $\Delta/t \ll 1$ case [see Fig. 1(a)]. Greater Δ/t also leads the nesting peaks to emerge at a lower threshold of ω/Δ , and more distinguished when they exist.

Some stray structures off \mathbf{Q}_{AF} always exist especially in the case of large Δ/t and ω/Δ . Their magnitude can be comparable or even larger than the IC structure, but

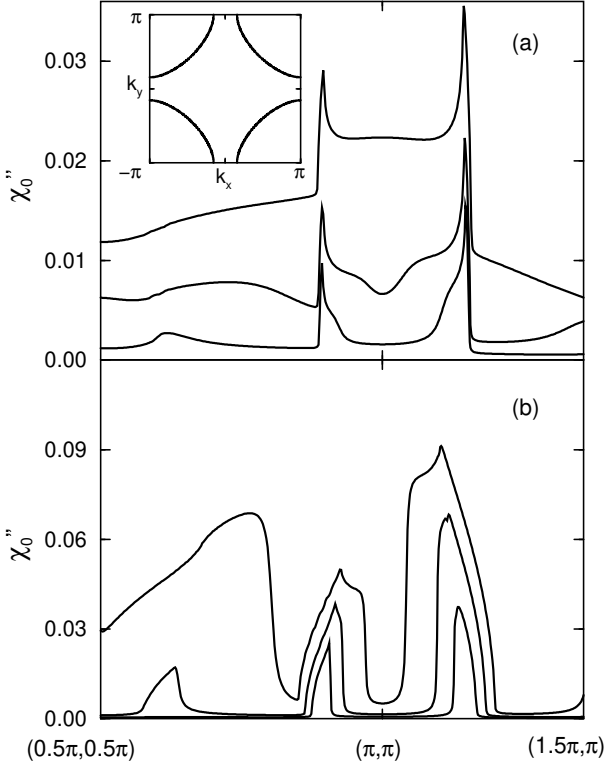


FIG. 1. Frequency evolution of the SC state $\chi''_o(\mathbf{q}, \omega)$ with different Δ/t is shown. For (a) $\Delta/t = 0.03$, $\omega/\Delta = 1.0, 1.5$, and 2.0 (from bottom to top); (b) $\Delta/t = 0.30$, $\omega/\Delta = 0.6, 1.0$, and 1.4 (from bottom to top). In (b), the broad peak shifts at changing frequency, and some stray structures away from \mathbf{Q}_{AF} is present. The RPA-correction [see Fig. 8(d)] makes the shifting more pronounced and those stray structures less prominent. For both panels, $T = 0$, the dispersion is $t = 1$, $t' = -0.25$, and $\mu = -0.65$. The FS centered at $\mathbf{k} = (0, 0)$ is shown in the inset and the plots are along $\mathbf{q} = (0.5\pi, 0.5\pi) - (\pi, \pi) - (1.5\pi, \pi)$.

when the RPA-correction is introduced they will become relatively weaker.

The most important of all, we have found that when the SC system is away from the limit $\Delta/v_F \ll \pi$ (modeled by $\Delta/t \ll 1$), the nesting peak is broad and could be driven by ω to shift. We will discuss in Sec. IV that the shift direction actually depends on the orientation of the curvature of the FS at the gap nodes. We can thus address the static IC peaks in LSCO by the limit $\Delta/v_F \ll \pi$, and the ω -shifted broad IC peak in YBCO at $\omega/\Delta < 2$, by a larger Δ/v_F and a nodal FS geometry resembles to that in Fig. 1(a).

B. Normal State

The normal state is described by $\Delta(T) = 0$, which leaves the bandwidth as the only energy scale, and no coherence factor. Eq. (1) is reduced to the Lindhard function

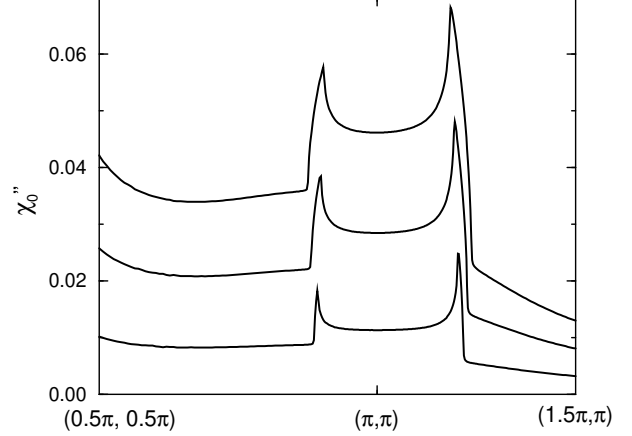


FIG. 2. Normal state $\chi''_o(\mathbf{q}, \omega)$ at $\omega/t = 0.04, 0.10$, and 0.16 (from bottom to top) is shown along $\mathbf{q} = (0.5\pi, 0.5\pi) - (\pi, \pi) - (1.5\pi, \pi)$. Such IC peaks exist only in the regime $\omega/t \ll 1$ [compare with a larger ω/t case shown in Fig. 3(b)]. Temperature $T = 0$ and the dispersion is $t = 1$, $t' = -0.25$, and $\mu = -0.65$.

$$\chi_o(\mathbf{q}, \omega) = \sum_{\mathbf{k}} \frac{f(\xi_{\mathbf{k}}) - f(\xi_{\mathbf{k}+\mathbf{q}})}{\omega - \xi_{\mathbf{k}} + \xi_{\mathbf{k}+\mathbf{q}} + i\Gamma}. \quad (5)$$

Its reduction from Eq. (1) will be letting $E_{\mathbf{k}} = |\xi_{\mathbf{k}}|$, $|\xi_{\mathbf{k}}| = \xi_{\mathbf{k}}$ and $-\xi_{\mathbf{k}}$ when $\xi_{\mathbf{k}} > 0$ and $\xi_{\mathbf{k}} < 0$ respectively. The relation $f(-\xi_{\mathbf{k}}) = 1 - f(\xi_{\mathbf{k}})$ is also used. It can also be derived from a normal system at the outset as well.

Figure 2 is the normal state spectra with the same dispersion as in Fig. 1. The IC peaks locate at the same places but exist only at $\omega/t \ll 1$. Before being destroyed, increasing frequency broadens the peak and enhances the intensity. Similar to previous subsection, $\omega/t \ll 1$ in our context could simply due to a steep dispersion at FS and does not necessarily imply a "small" frequency.

Spectra in normal states resemble those of $\omega/\Delta > 2$ in SC state simply because normal states correspond to the limit $\Delta \rightarrow 0$ and hence $\omega/\Delta \rightarrow \infty$. The IC peaks in the normal state only exist at $\omega/t \ll 1$, i.e. $\omega/v_F \ll \pi$ and static in location.

C. Transition between Superconducting and Normal States

We have studied the SC phase and normal phase. Now we consider a continuously running gap driven by temperature, and this is essentially to study the effect of the growth of the coherence factor and allowed transitions in phase space with the SC gap. We will take an empirical relation $\Delta(T) = \Delta(0)[1 - (T/T_c)^{41/2}]$ [see inset in Fig. 3] at $T < T_c$ in our discussion.

If the IC peaks exist in the normal state, at entering the SC state [see Fig. 3(a)] it will be enhanced when $\omega/\Delta(0) > 1$ and suppressed if $\omega/\Delta(0) \sim 1$, and it will also be sharpened for $\omega/\Delta(0) < 2$ since spectral weight at \mathbf{Q}_{AF} will be gapped out.

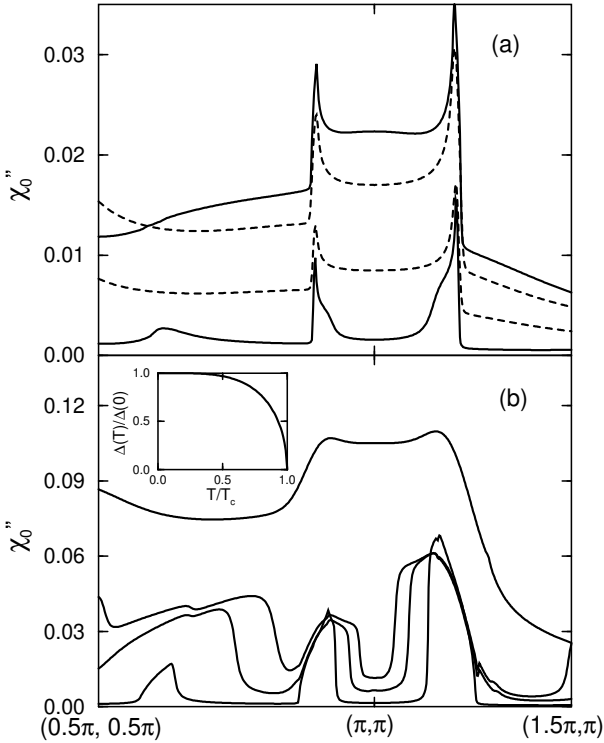


FIG. 3. Bare spectra $\chi''_o(\mathbf{q}, \omega)$ with different $\Delta(0)/t$ and $\omega/\Delta(0)$ at varying temperature. (a) For $\Delta(0)/t = 0.03$, the solid lines show the $T = 0$ spectra at $\omega/\Delta(0) = 1.0$ and 2.0 (from bottom to top). Likewise frequencies for the dashed lines but with $T = T_c = 0.25\Delta(0)$. (b) For $\Delta(0)/t = 0.30$ and $\omega/\Delta(0) = 1.0$, $T/T_c = 0, 0.80, 0.85$, and 1.0 (from bottom to top). $T_c = 0.25\Delta(0)$ and the inset shows the assumed T -dependence of $\Delta(T)$. Heating up converges the IC peak cluster in (b) to commensurate at $T \lesssim T_c$. This behavior is more conspicuous when the RPA-correction is included [see Fig. 11(b)]. The dispersion used in both panels is $t = 1$, $t' = -0.25$, and $\mu = -0.65$. The plots are along $\mathbf{q} = (0.5\pi, 0.5\pi) - (\pi, \pi) - (1.5\pi, \pi)$.

Figure 3(b) shows a non-trivial case of transition across T_c . It shows that the frequency-shifted peak [see Fig. 1(b)] will also be temperature shifted, and necessarily vanishes in the normal state. By increasing temperature, the well-defined IC peaks at low temperature are continuously broadened, shifted towards \mathbf{Q}_{AF} , and merge into broad commensurate (or weakly IC structure) in the normal state. The change is mild at $T < T_c/2$ where $\Delta(T)$ is almost constant, and is drastic at $T \lesssim T_c$ since $\Delta(T)$ is rapidly changing. We will come back to this at Sec. VI.

The limit $\Delta/t \ll 1$ appropriate for LSCO is in congruence with the limit $\omega/t \ll 1$ for ω at the order of Δ , and thus preserves the peak into the normal state. The frequency- and temperature-shifted peak in SC state necessarily violates the limit $\omega/t \ll 1$ and implies absence of the peak in normal state, which describes the case of YBCO.

IV. EXCITATION AT BARE LEVEL — THE DYNAMIC LOCAL NESTING

The IC peaks are originated from the *umklapp* and inversion symmetry of the dispersion. This section is devoted to the discussion of the properties of the bare excitation mentioned in Sec. III. It is found that both the ω - and T -driven peak shifting effect are due to the dynamic and local nature of the nesting effect. We illustrate the mechanism by a zero temperature SC system and discuss the effect of finite temperature and normal state later.

The bare spectrum of a zero temperature SC system is given by

$$\chi''_o(\mathbf{q}, \omega) = \frac{\pi}{4} \sum_{\mathbf{k}} \left[1 - \frac{\xi_{\mathbf{k}} \xi_{\mathbf{k}+\mathbf{q}} + \Delta_{\mathbf{k}} \Delta_{\mathbf{k}+\mathbf{q}}}{E_{\mathbf{k}} E_{\mathbf{k}+\mathbf{q}}} \right] \times [\delta(\omega - E_{\mathbf{k}} - E_{\mathbf{k}+\mathbf{q}}) - \delta(\omega + E_{\mathbf{k}} + E_{\mathbf{k}+\mathbf{q}})]. \quad (6)$$

The integrand consists of a coherence factor which reflects the non-time-reversal invariance nature of the magnetic measurement, and a δ -function that imposes the energy conservation rule.

The role of the δ -function should be first discussed since it is the most dominant. It limits the contributing region of the phase space by the energy conservation $E_{\mathbf{k}} + E_{\mathbf{k}+\mathbf{q}} = \omega$. At $\omega \sim 0$, the only possibility is $E_{\mathbf{k}}$ and $E_{\mathbf{k}+\mathbf{q}}$ both ~ 0 . Therefore \mathbf{q} can only be vectors connecting the gap nodes, which are $\mathbf{Q}_{\delta_o} \equiv (\pi + \delta_o, \pi \pm \delta_o)$ and $(\pi - \delta_o, \pi \pm \delta_o)$, with $\delta_o = 2 \sin^{-1} \sqrt{[t - \sqrt{t^2 - t'^2} \mu] / [-2t']}$.

At $\omega > 0$, to satisfy $E_{\mathbf{k}} + E_{\mathbf{k}+\mathbf{q}} = \omega$, \mathbf{q} can be any momentum that connects points on the contours $E_{\mathbf{k}} = \omega_1$ and $E_{\mathbf{k}+\mathbf{q}} = \omega_2$, if $\omega_1 + \omega_2 = \omega$. These are strips of area stretched out from the gap node along the FS. For most \mathbf{q} , it only constitutes a featureless and “incoherent” background in the \mathbf{q} -space. To constitute a salient structure out of the background one needs to have extra factors that can stack extra weight onto the background. A situation that can further provide some weight is when $\omega_1 = \omega_2 = \omega/2$ and all the two frequency dependent contours become $E_{\mathbf{k}} = E_{\mathbf{k}+\mathbf{q}} = \omega/2$. It spans the whole FS when $\omega \rightarrow 2\Delta$. Now \mathbf{q} can “nest” two contours locally by passing through points $\mathbf{k}_o = (m\pi, n\pi)$ (where m and n are integers) in the BZ. It occurs because the ω -dependent contour is always locally parallel at $\mathbf{k}_o + \mathbf{k}$ and $\mathbf{k}_o - \mathbf{k}$ due to the dispersion $E_{\mathbf{k}}$ has the $\mathbf{k} \leftrightarrow -\mathbf{k}$ inversion and *umklapp* symmetry in the extended BZ. This nesting is thus *dynamic* and *local*.

As an example, we consider $\chi''_o(\mathbf{q}, \omega)$ at $\mathbf{q} \in [0 \sim 2\pi, 0 \sim 2\pi]$ and the integration over \mathbf{k} in evaluating χ''_o is run over $(k_x, k_y) \in [-\pi \sim \pi, -\pi \sim \pi]$. Fig. 4 illustrates the local-nesting at a frequency $\omega < 2\Delta$. In the integration over the first quadrant $(k_x, k_y) \in [0 \sim \pi, 0 \sim \pi]$, those local nesting vectors are shown as \mathbf{q}_I . Likewise,

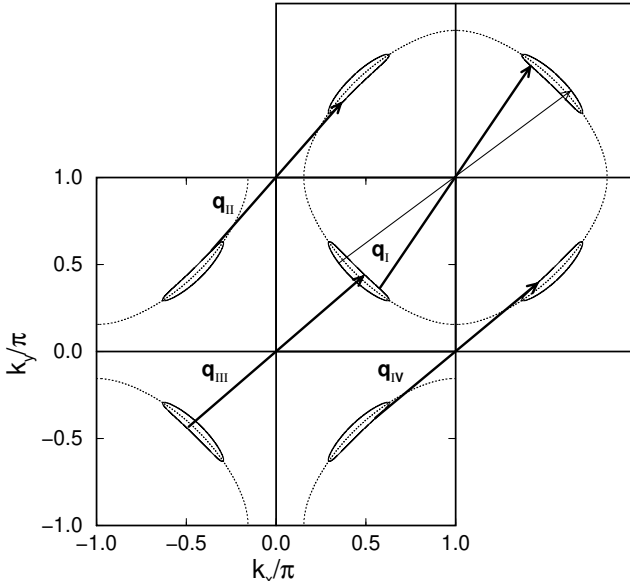


FIG. 4. Energy contour $E_{\mathbf{k}} = \omega/2$ in the extended BZ for $\omega = 1.0\Delta(0)$. Some arbitrary local-nesting vectors \mathbf{q}_I , \mathbf{q}_{II} , \mathbf{q}_{III} , and \mathbf{q}_{IV} are shown. The thick vector between above-FS contour piece have better nesting due to the smaller curvature. The FS is shown as dotted line, and the dispersion is $t = 1$, $t' = -0.25$, and $\mu = -0.65$. The gap is chosen as $\Delta/t = 0.50$ for clarity in illustration.

\mathbf{q}_{II} for the second, \mathbf{q}_{III} for the third, and \mathbf{q}_{IV} for the fourth quadrant.

Figure 5(a) illustrates the consequence of such local-nesting effect, the ridge-like structure of $\chi''_o(\mathbf{q}, \omega)$ in \mathbf{q} -space. The formation of the structure can be illustrated by an illuminating calculation, where the integration is done only over the first quadrant $(k_x, k_y) \in [0 \sim \pi, 0 \sim \pi]$. Then only one branch of ridge is obtained [see Fig. 5(b)] and its orientation is the same as the contour in quadrant $(k_x, k_y) \in [\pi \sim 2\pi, \pi \sim 2\pi]$. The ends of the ridge are determined by $\Delta_{\mathbf{k}} = \omega/2$. The ridge locus in \mathbf{q} -space resembles the locus of the contour (which is approximately the FS) in \mathbf{k} -space but have twice the extension since the nesting vectors are twice the vectors describing the locus of the FS in \mathbf{k} -space [see Fig. 4].

An IC peak is a result of overlapping of two ridges at the symmetrical points $\mathbf{Q}_{\delta} = (\pi, \pi \pm \delta)$ and $(\pi \pm \delta, \pi)$, where $\delta = 2\sin^{-1}[-\mu/(2t)]$, when $\omega > \omega_{\delta} \equiv \Delta(T)[- \mu/(2t)]$. For those FS of open topology [see Fig. 4], the ridges overlap also at $\mathbf{Q}_{\delta'} = (\pi + \delta', \pi \pm \delta')$ and $(\pi - \delta', \pi \pm \delta')$ when $\omega > \omega_{\delta'} \equiv \Delta(T)\sqrt{\mu/t'}$, where $\delta' = 2\sin^{-1}\sqrt{\mu/(4t')}$. It should be reminded that the analytical form given above either for δ_o , δ , or δ' is exact only when $\Delta/t \rightarrow 0$. For $\Delta/t > 0$ the peak has a thickness and the location of its apex may depend on other factors.

Frequency $\omega_{\delta'} \equiv \Delta(T)\sqrt{\mu/t'}$ is also the onset frequency of $\chi''_o(\mathbf{Q}_{AF}, \omega)$, since \mathbf{Q}_{AF} also connects equivalent points of $\mathbf{Q}_{\delta'}/2$ (also called the “hot spots”).

Due to the bending of the ridges [see Fig. 5], one will

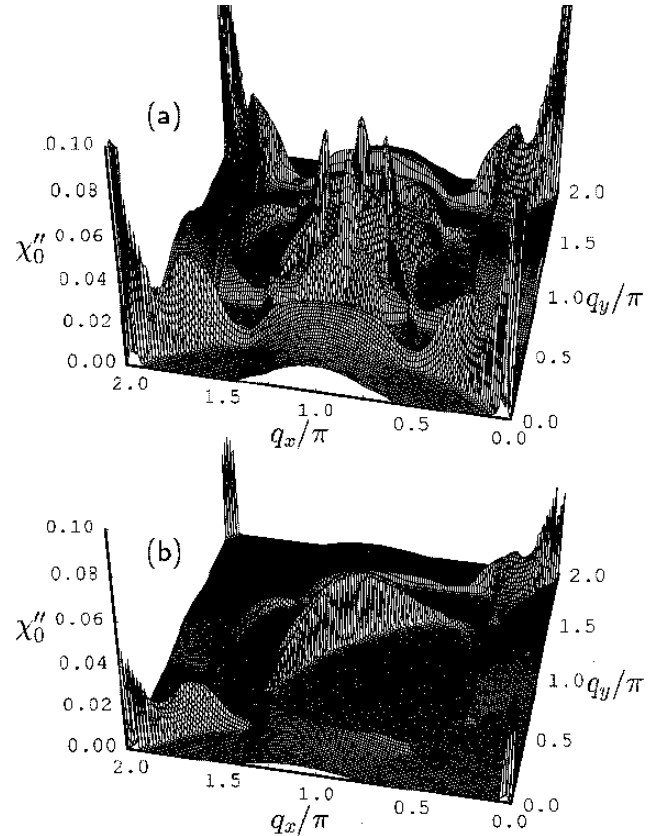


FIG. 5. (a) A bare spectrum $\chi''_o(\mathbf{q}, \omega)$ in the full \mathbf{q} -space at $\omega = 1.0\Delta(0)$. (b) a single branch of “ridge”, obtained when the integration over \mathbf{k} in Eq. (1) is done only over the quadrant $(k_x, k_y) \in [0 \sim \pi, 0 \sim \pi]$. Four of these 90-degree rotated branches superpose to give $\chi''_o(\mathbf{q}, \omega)$ in (a). Refer the dispersion parameters to Fig. 1(b).

miss the nodal excitation point \mathbf{Q}_{δ_o} if one scan two nesting IC peaks at \mathbf{Q}_{δ} in their nearest distance direction. Therefore χ''_o will be seen as always gapped at any \mathbf{q} . Since this should be more prominent when Δ/t is small (which is the case in LSCO), this may explain the observation of a momentum independent spin gap by Lake *et al.* on LSCO [5].

A very peculiar feature which has been overlooked previously is the peak shifting behavior, brought by the slight difference of curvature of the contour pieces below and above the FS near the gap nodes (which is the FS segment that determines the properties of the IC peak at \mathbf{Q}_{δ}). This occurs when the nodal FS segment has nonzero curvature and the contour $E_{\mathbf{k}} = \omega/2$ is appreciably opened up from it. In the geometry of FS shown in Fig. 4, the above-FS contour has a smaller curvature and can be nested more effectively. That causes the ridges to have a biased cross-section profile higher at one side, and this feature necessarily is retained in the nesting peaks that have their apex biased to one side [see Fig. 1(b) and Fig. 5]. The opening up of the contour also gives the ridges and peaks widths that grow with ω . As ω in-

creases, the apex of peaks are shifted due to the increase of peak widths [see Fig. 1(b)]. The broad and shifting behavior of the bare excitation peak are thus necessarily coexist.

Finite temperature in SC states drives the gap and thus changes the extensions of ridges both along and away from the FS. When T broadens the ridges away from FS, it simultaneous shifts the peaks apex like increasing ω . Besides, T always causes some smearing in all cases, the SC or the normal state.

When the dispersion at FS is steep or the gap is small (i.e. $\Delta/v_F \ll \pi$ or $\Delta/t \ll 1$), the contours are confined strictly on the FS and hence the ridges and IC peaks formed are slim and no shift of peak is possible. The peak will also not shifted when there is null curvature of the FS because there is no difference of curvature between the above- and below-FS contours.

The coherence factor has values between 0 and 2, and that can provide modification of the intensity as pointed out in the literature. The condition $\xi_{\mathbf{k}} \rightarrow 0$ at the FS tends to maximize the spin coherence factor to 2 at $\Delta_{\mathbf{k}}\Delta_{\mathbf{k}+\mathbf{q}} < 0$, and minimize it to 0 at $\Delta_{\mathbf{k}}\Delta_{\mathbf{k}+\mathbf{q}} > 0$. As our nesting vectors has $\Delta_{\mathbf{k}}\Delta_{\mathbf{k}+\mathbf{q}} > 0$, the ends of ridges are smoothly suppressed by the cutoff $\Delta_{\mathbf{k}} = \omega/2$. In the case of larger Δ/t , the condition $\xi_{\mathbf{k}} \rightarrow 0$ is not well satisfied at finite ω/Δ since the contour is opened up appreciably from the FS. This weakens the suppression effect before cutoff, and the ridges will overlap at more sizable values and gives a higher contrast of the nesting IC peaks. It also lowers the threshold ω/Δ for the emergence of the peaks.

The normal state is the lift of the energy restriction by the gap, and the disappearance of coherence factor. The ridges now always span the whole \mathbf{q} -space and the nesting peaks always exist in principle. But due to replacing a stronger energy constraint (due to two-particle excitation) by a looser constraint (due to one-particle excitation), the transition now floods over regions far away from the FS and makes the widths of ridges dispersed and the nesting peaks less distinguishable. Especially now the transition near \mathbf{Q}_{AF} is filled high for hole-like FS.

Albeit the underlying cause of formation of the ridges and nesting peaks (*umklapp* and \mathbf{k} -inversion symmetry) is irrelevant to the existence or not of the SC gap, there are still some upper limits on ω/Δ or ω/t for the IC peaks to exist. Since increasing ω/t broadens the ridges, the ridge and peak structure will be always destroyed at very high ω/t . The same is true for very high T/t where the excitation is deconfined from the FS. It is easier for the peak to survive in the SC state because the near \mathbf{Q}_{AF} transition is kept away at $\omega/\Delta < 2$ [see Fig. 3(b)].

To summarize, the IC peaks in principle should exist at low ω/t and T/t in any state, and any band with *umklapp* and inversion ($\mathbf{k} \leftrightarrow -\mathbf{k}$) symmetry. The nesting peak in the SC state can be driven by ω or T to shift if it is broad and at the meantime the nodal FS has nonzero curvature. In Sec. VI, the existence of near Fermi level

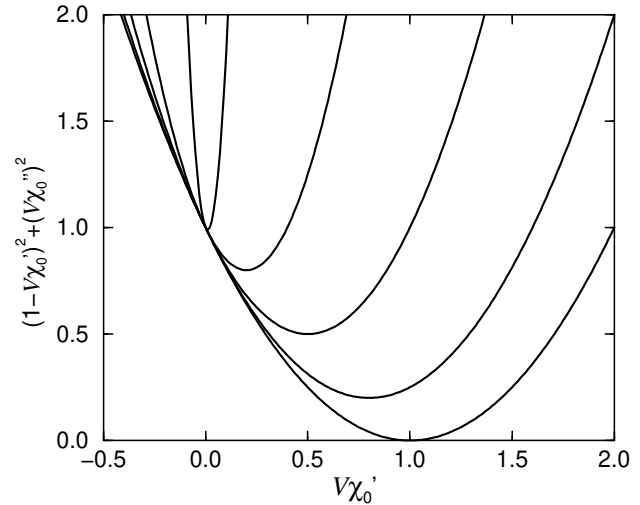


FIG. 6. The Stoner factor $[(1 - V\chi'_o)^2 + (V\chi''_o)^2]$ is plotted against $V\chi'_o$ for $V\chi''_o/\chi'_o = 0, 0.5, 1.0, 2.0$, and 10 (from bottom to top).

vHS at \overline{M} which leads to opposite ω -driven incommensuration evolution at different frequency regime will be discussed.

V. RPA-CORRECTED EXCITATION

The RPA-correction has two possible consequences, the scaling effect and the occurrence of resonance. In this section we study their general properties and the scaling effect in detailed. We leave the study of an important resonance, the commensurate peak to Sec. VI.

The RPA-renormalized spectrum is

$$\chi''(\mathbf{q}, \omega) = \frac{\chi''_o(\mathbf{q}, \omega)}{[1 - V_{\mathbf{q}}\chi'_o(\mathbf{q}, \omega)]^2 + [V_{\mathbf{q}}\chi''_o(\mathbf{q}, \omega)]^2}. \quad (7)$$

It can be viewed as a scaling of χ''_o by the positive denominator $[(1 - V_{\mathbf{q}}\chi'_o)^2 + (V_{\mathbf{q}}\chi''_o)^2]$ which is quadratic in $V_{\mathbf{q}}$. This scaling factor is sometimes called the Stoner factor.

Figure 6 shows that Stoner factor $[(1 - V\chi'_o)^2 + (V\chi''_o)^2]$ has always a minimum less than 1 and no maximum. It is less than 1 when $V\chi'_o$ lies between 0 and $2/[1 + (\chi''_o/\chi'_o)^2]$. Given χ_o , it is minimized by V equals to

$$V_m = \frac{1}{\chi'_o} \cdot \frac{1}{1 + \left[\frac{\chi''_o}{\chi'_o} \right]^2}. \quad (8)$$

The corresponding maximized χ'' then equals to

$$\chi''_m = \chi''_o \cdot \left[1 + \left[\frac{\chi'_o}{\chi''_o} \right]^2 \right]. \quad (9)$$

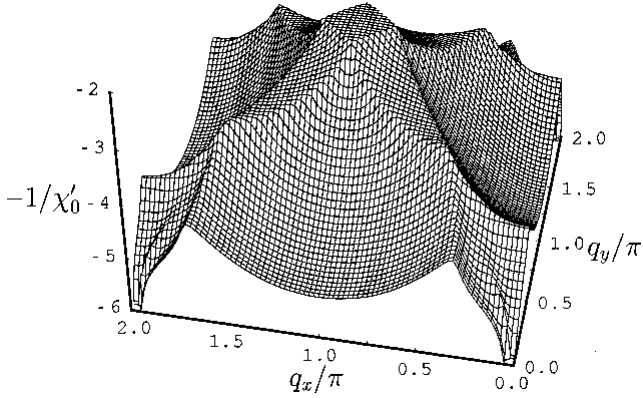


FIG. 7. A typical SC state $-1/\chi'_o(\mathbf{q}, \omega = 0)$ in the full \mathbf{q} -space. The no-instability bound of the interaction strength is $V_{\mathbf{q}} < 1/\chi'_o(\mathbf{q}, \omega = 0)$. For $V_{\mathbf{q}} = J_{\mathbf{q}}$, $|J| < 1/\chi'_o(\mathbf{q} \sim \mathbf{Q}_{AF}, \omega = 0) \simeq 2.2$. The plot has $T = 0$, $\Delta/t = 0.03$, and band dispersion $t = 1$, $t' = -0.25$, and $\mu = -0.65$.

Thus the maximum enhancement factor is $[1 + (\chi'_o/\chi''_o)^2]$. The locus of minima of the Stoner factor in Fig. 6 follows $\chi''_o/\chi''_m + \chi'_o V_m = 1$.

There are two limiting cases. When $\chi''_o/\chi'_o \gg 1$, the maximum enhancement factor is $\simeq 1$ and occurs at $V \simeq \chi'_o/\chi''_o^2 \rightarrow 0$, which means no enhancement but suppression of χ''_o for any V . In the case of $\chi''_o/\chi'_o \sim 0$, the maximum enhancement factor $\simeq (\chi'_o/\chi''_o)^2$ diverges χ''_o to infinity at $1 - V\chi'_o = 0$. This is the resonance of the corresponding spin collective mode with damping χ''_o .

These properties of the RPA-correction dictates the physical regime of the interaction strength $V_{\mathbf{q}}$ in a system. Since damping χ''_o is always null at $\omega = 0$, $1 - V_{\mathbf{q}}\chi'_o(\mathbf{q}, \omega = 0) = 0$ causes instability in the system and therefore sets a bound for physical $V_{\mathbf{q}}$ by requiring $1 - V_{\mathbf{q}}\chi'_o(\mathbf{q}, \omega = 0) > 0$ [e.g. see Fig. 7]. A stable system should have $V_{\mathbf{q}}$ stay sufficiently away from the instability boundary.

When there is no sufficiently strong influence sources such as a band singularity near FS, $\chi''_o(\mathbf{q}, \omega)$ changes smoothly with ω . Due to χ_o is a causal function and χ'_o and χ''_o are related by the Kramers-Kronig relation, $\chi'_o(\mathbf{q}, \omega)$ will then be inert to ω change. For the case of always well-defined IC peaks as in the case of LSCO, ω/t should be always small [see Sec. IV] and that leads to a quiescent $\chi'_o(\mathbf{q}, \omega)$ at $\omega/\Delta < 2$ [see Fig. 8(a)]. Absence of zero- ω instability almost guarantees absence of nonzero- ω resonance, and that keeps the RPA-correction in the scaling regime where all features of χ''_o resembles χ'_o . In conclusion, the well-defined and static IC peaks in wide ranges of frequency and temperature infers a small possibility of RPA-resonance, and this may explain why LSCO has no commensurate resonance in contrast to YBCO.

Some typical no-resonance RPA spectra χ'' of SC systems are shown in Fig. 8. An AF interaction $J_{\mathbf{q}}$ of moderate strength is considered. In general, the structures

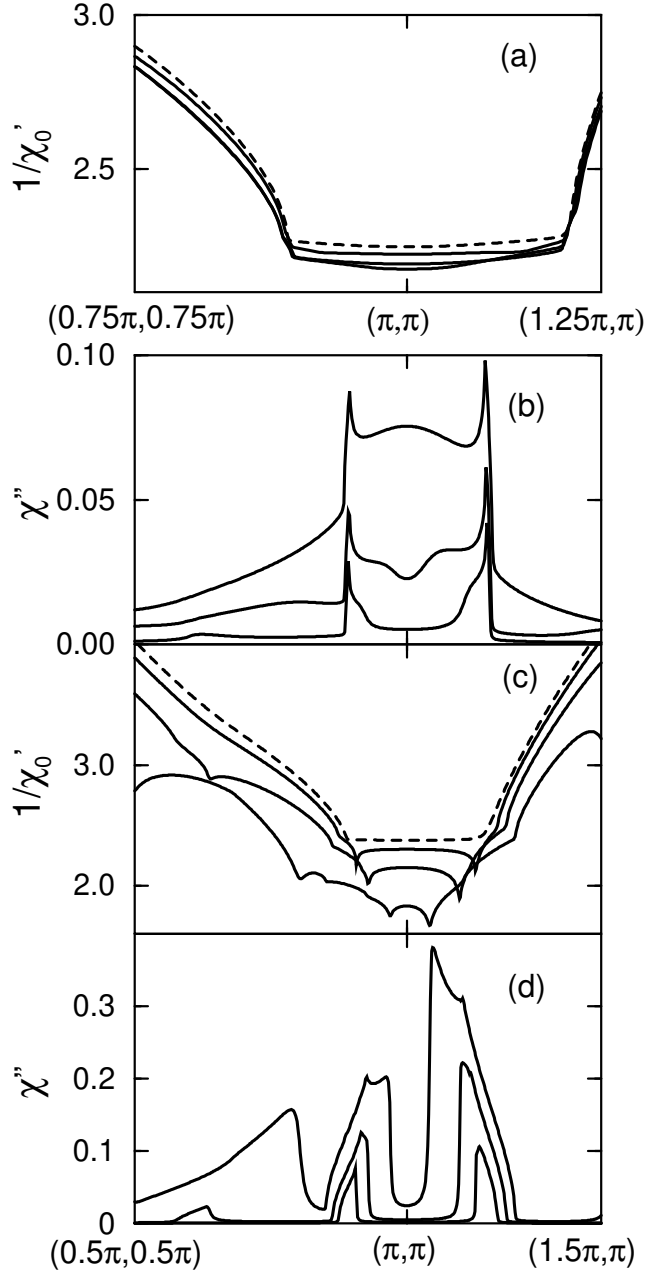


FIG. 8. RPA effect on small and larger Δ/t systems. The AF interaction here with $|J|/t = 1.0$ is in the scaling regime. All graphs except (a) are plotted along $\mathbf{q} = (0.5\pi, 0.5\pi) - (\pi, \pi) - (1.5\pi, \pi)$. For $\Delta/t = 0.03$ case, (a) $1/\chi'_o(\mathbf{q}, \omega)$ [along $\mathbf{q} = (0.75\pi, 0.75\pi) - (\pi, \pi) - (1.25\pi, \pi)$] at $\omega/\Delta = 0$ (dashed line), 1.0, 2.0 and 1.5 (solid lines at \mathbf{Q}_{AF} from top to bottom). Its robustness at the change of ω infers small chance of RPA-resonance within $\omega < 2\Delta$. Correspondingly, (b) $\chi''(\mathbf{q}, \omega)$ at $\omega/\Delta = 1.0, 1.5$ and 2.0 (from bottom to top). For $\Delta/t = 0.30$ case, (c) $1/\chi'_o(\mathbf{q}, \omega)$ at $\omega/\Delta = 0$ (dashed line), 0.60, 1.0 and 1.4 (solid lines from top to bottom). Correspondingly, (d) $\chi''(\mathbf{q}, \omega)$ at $\omega/\Delta = 0.6, 1.0$ and 1.4 (from bottom to top). Due to the local minima in $1/\chi'_o$, those peaks in (d) are sharpened and have more spectacular shifting. Temperature $T = 0$ and the corresponding bare spectra were shown previously in Fig. 1.

near \mathbf{Q}_{AF} is brought out more salient [compare Fig. 8 to Fig. 1], due to both the local positivity of $J_{\mathbf{q}}$ and smaller $1/\chi'_o$ near \mathbf{Q}_{AF} . The SC state $1/\chi'_o$ at small ω/Δ is smaller at $\sim \mathbf{Q}_{AF}$ because it is close to the nodal excitation. The figure also shows an important feature in the case of larger Δ/t , sharp local minima of $1/\chi'_o$ induced by χ''_o always exist just at the sharp edges of the bare IC peaks. This results in sharpened peaks in χ'' and more conspicuous converging behavior. Besides, the surging around of structures in χ''_o also agitates much activity in χ'_o at all over \mathbf{q} -space. There is not much difference between the AF and Hubbard vertex correction, except that the AF correction selectively affects the excitation near \mathbf{Q}_{AF} .

To conclude this section, the RPA-correction gives \mathbf{q} -dependence scaling of spectral weight distribution if not resonance that qualitatively changes the spectrum. In this section we have studied the scaling regime and it is found that it makes structures away from \mathbf{Q}_{AF} less prominent and peak shifting behavior (when it exists) more salient. The appropriate description of LSCO, the small Δ/t limit which gives robust IC peak against various changes [see Sec. III] infers unlikelihood of RPA resonance.

VI. EXCITATION SPECTRUM AND \overline{M} -POINT VAN HOVE SINGULARITY

This is a RPA theory of spin excitation with both commensurate and IC excitation, and it turns out to have a good agreement with the recently reported data on YBCO. Those qualitative behaviors of the observed spectrum actually already have resided in χ''_o , and difference between the bare and RPA theories only appears in finer comparisons, such as the recent data on temperature variation [2]. The experimentally observed approaching of the 1-dimensional *extended*-saddle-vHS at $\overline{M} = (0, \pi)$ to the Fermi level [21,24] is here mimic by a shallow 2-dimensional simple saddle-vHS at \overline{M} . This simple saddle-vHS is taken for the sake of simplicity, and it is believed that it has captured the essence into a RPA theory. Nevertheless its extended nature is shown recently [26] to be crucial in the quantitative comparison between a bare theory and experiments.

A number of comprehensive theories including both commensurate and IC excitation [12,13,26,14–16] were explored since the discovery of the behavior in YBCO. It is important to note that all of them are Fermi-liquid based in one form or another, and most of them are RPA theories [12,13,15,16]. The possibility of a bare theory was investigated by Abrikosov [26,27] and us [14]. The commensurate peaks obtained from χ''_o are in general weaker, broader, and occurs at $\omega_o \gtrsim 2\Delta$, which is in contrast to the much stronger and sharper one in χ'' that occurs at $\omega_o < 2\Delta$. However, recently it has been shown that a bare theory incorporating the extended-vHS [26]

gives reasonable agreement in peaks intensity and width to the experiments. Attempting to rely on the criterion $\omega_o \gtrsim 2\Delta$ or $\omega_o < 2\Delta$ to choose an appropriate description also encounters the subtleties in the determination of the SC gap. The complication is especially pronounced in the underdoped side to which there is still controversies as whether the SC gap and the pseudogap are the same gap [28–30]. Therefore in some cases $\omega_o \gtrsim 2\Delta$ seems to be favored (see discussion in Ref. [27]), while in other cases $\omega_o < 2\Delta$ is preferred (e.g. in the underdoped). As a result we believe that at present there is no clear evidence to favor over either the bare or the RPA scenario. While the commensurate peak had received much attention in the past few years, recently the focus has been switched to the frequency-shifted IC peaks since the discovery. All the present scenarios are based on the FS nesting effect, which depends mainly on the nodal FS, except the one recently proposed by Abrikosov [26] which relies on the band mass at the extended-vHS region. The discussion of the temperature-shifted IC peaks has been still missing from the literature.

On the possibility of the presence of an collective resonance at \mathbf{Q}_{AF} , since any susceptibility function or interaction vertex on the lattice is symmetric under the transformation $\mathbf{Q}_{AF} + \delta\mathbf{q} \rightarrow \mathbf{Q}_{AF} - \delta\mathbf{q}$ as dictated by the lattice symmetry, they have extrema at \mathbf{Q}_{AF} and at some interaction strength, $1 - V\chi'_o = 0$ at \mathbf{Q}_{AF} out of its vicinity. A resonance appears if damping $\chi''_o \sim 0$. It was pointed out in Sec. V that for systems with well-behaved properties near FS, resonance can occur only at interaction strengths close to the instability boundary. In this section we proceed to show that the SC state with the vHS at \overline{M} close to the Fermi level introduces singularity into the $\chi_o(\mathbf{Q}_{AF}, \omega)$ and thus enhances the chance of resonance at lower interaction strengths.

The dispersion here taken to mimic the YBCO or BSCCO dispersion has a topologically-opened (hole-like) FS and a simple saddle-vHS at \overline{M} situated closely beneath the Fermi level, $\xi_{\mathbf{k}=\overline{M}}/\Delta = -0.5$. The recent report of an electron-like FS in BSCCO [31] will not change our conclusion as long as $|\xi_{\mathbf{k}=\overline{M}}|/\Delta$ is small. The interaction is taken as $J_{\mathbf{q}}$, with $|J|/t = 1.6$ which gives a commensurate resonance at $\omega/\Delta = 1.5$. The zero temperature $1/\chi'_o$ and RPA spectrum in momentum space are shown in Fig. 9 at different frequencies. The minimum of $1/\chi'_o(\mathbf{Q}_{AF}, \omega)$ occurs at $\omega/\Delta = 1.77$, which is just at the stepwise onset of $\chi''_o(\mathbf{Q}_{AF}, \omega)$.

Away from the resonance the RPA correction is in the scaling regime [see Fig. 9] as discussed in Sec. V. An important consequence of the existence of shallow vHS at \overline{M} is the presence of a diverging-incommensurability IC structure at increasing frequency at $\omega > \omega_o(T=0)$. This behavior has the same origin as the converging incommensurability at $\omega \rightarrow \omega_o$ from below. Owing to the shallow flat band at \overline{M} , the nesting contours $E_{\mathbf{k}} = \omega/2$ at high frequencies necessarily have smaller curvature at the segments below FS, and can be locally nested more effectively [see Fig. 10]. The IC peak profile in this

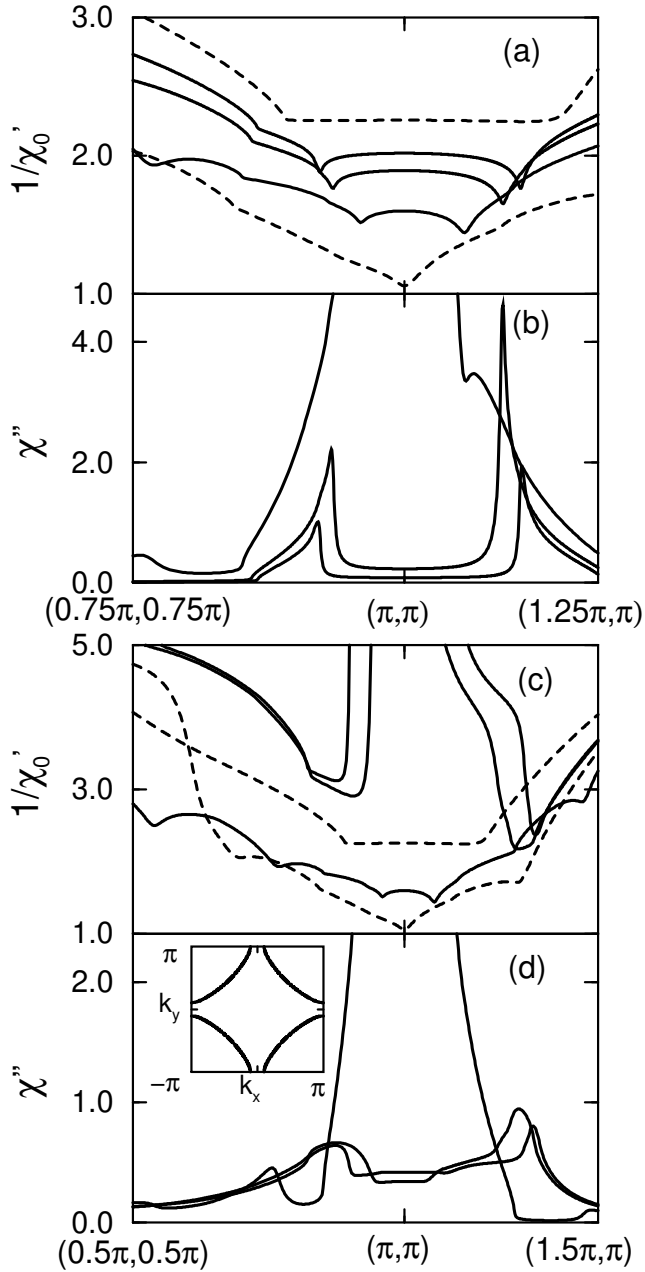


FIG. 9. Frequency-driven peak shifting at different frequency regimes : (a) $1/\chi'_0(\mathbf{q}, \omega)$ at $\omega/\Delta = 1.0, 1.2$, and 1.5 [solid lines from top to bottom]; (b) $\chi''(\mathbf{q}, \omega)$ at $\omega/\Delta = 1.0, 1.2$, and 1.5 [at decreasing incommensurability along $(\pi, \pi) - (1.25\pi, \pi)$]. (c) $1/\chi'_0(\mathbf{q}, \omega)$ at $\omega/\Delta = 1.5, 2.3$, and 2.5 [solid lines at increasing “incommensurability” of the minima along $(\pi, \pi) - (1.5\pi, \pi)$]; (d) $\chi''(\mathbf{q}, \omega)$ at $\omega/\Delta = 1.5, 2.3$, and 2.5 [at increasing incommensurability along $(\pi, \pi) - (1.5\pi, \pi)$]. The dashed lines from top to bottom in (a) and (c) show $1/\chi'_0$ at $\omega/\Delta = 0$ and 1.77 . χ'' in any case is calculated with $|J|/t = 1.6$ and the commensurate resonance occurs at $\omega = \omega_o(T = 0) = 1.5\Delta(0)$. We have truncated the strong commensurate peak for obvious reason. $T = 0$, the quasiparticle dispersion is $t = 1$, $t' = -0.20$, $\mu = -0.65$, and $\Delta = 0.30$ (gives $\xi_{\mathbf{k}=\overline{M}}/\Delta = -0.5$). The inset shows the FS centered at $\mathbf{k} = (0, 0)$. The broadening taken for all the calculations in this section is $\Gamma/t = 0.008$.

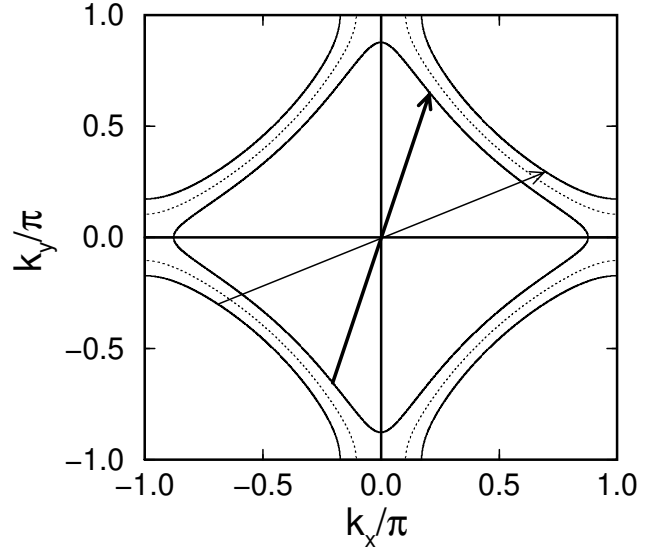


FIG. 10. Energy contour $E_{\mathbf{k}} = \omega/2$ in the reduced BZ for $\omega = 2.5\Delta(0) > \omega_o(T = 0)$. The arbitrarily shown thick local-nesting vector between below-FS contour has more pronounced nesting effect (compared to the thin vector) due to the smaller curvature. The FS is indicated as dotted line, and the dispersion is referred to Fig. 9.

regime is weaker because the below- and above-FS contours are too far apart to coherently form a ridge. The IC structures are always made more salient by the RPA-correction since a shifting peak in χ''_o always induces a local minimum in $1/\chi'_o$ with it.

Replacing the saddle-vHS by an extended-saddle-vHS do not affect the IC excitation at $\omega < \omega_o$ since only the nodal FS is of concern in this frequency regime. The diverging IC peaks at $\omega > \omega_o$ will be also expected to retain since the switch-over of the smaller and larger curvature of energy contour also should occur.

The larger amplitude of the change in $1/\chi'_o$ at $\omega/\Delta < 2$ is a result of the larger jump at the onset of $\chi''_o(\mathbf{Q}_{AF}, \omega)$ at $\omega_{\delta'} \equiv \Delta(T)\sqrt{\mu/t'} = 1.8\Delta(T)$. The onset is sharp due to the scattering is enhanced by the spin coherence factor at $\Delta_{\mathbf{k}}\Delta_{\mathbf{k}+\mathbf{Q}_{AF}} < 0$, and is more pronounced when Δ/t is large, while vanishes in the normal state. Besides the coherence factor, the enumeration of $\chi''_o(\mathbf{q}, \omega)$ in Eq. (6) also involves a δ -function which associates with the density of states at the transition regions. As the vHS at \overline{M} (at a depth of $\xi_{\mathbf{k}=\overline{M}} = 4t' - \mu$) comes close to the FS, it augments the onset jump in $\chi''_o(\mathbf{Q}_{AF}, \omega)$ and thus the divergence in $\chi'_o(\mathbf{Q}_{AF}, \omega)$. It is expected that the effect will be more pronounced if the 2-dimensional saddle-vHS is replaced by a realistic 1-dimensional extended-saddle-vHS. This widens the window and also lowers the threshold for the interaction strength giving resonance. When ω is increased to beyond the peak in $\chi''_o(\mathbf{Q}_{AF}, \omega)$, $1/\chi'_o(\mathbf{Q}_{AF}, \omega)$ recedes from zero rapidly and effectively turns off the RPA effect at \mathbf{Q}_{AF} [see Fig. 6]. Since the onset frequency manifestly scales with $\Delta(T)$, commensu-

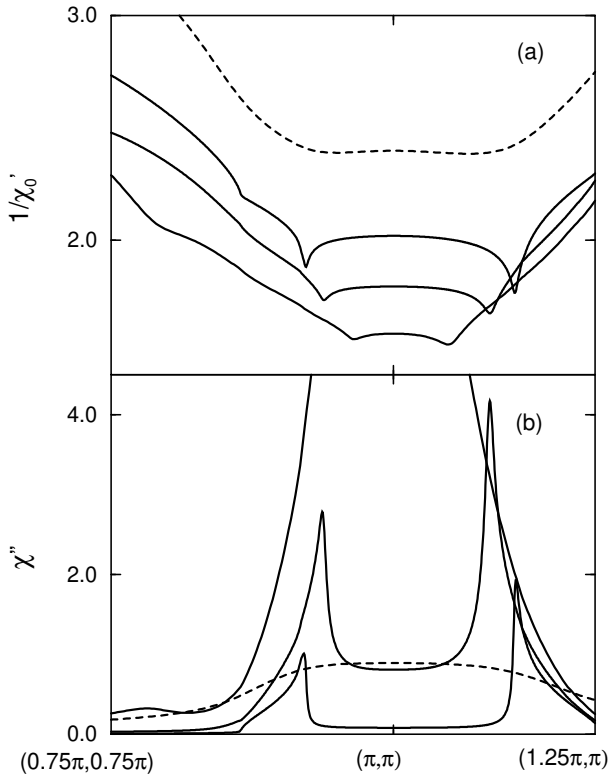


FIG. 11. Temperature-driven peak shifting at low frequency regime : At $\omega = 1.0\Delta(0) < \omega_o(T = 0)$, (a) $1/\chi'_o(\mathbf{q}, \omega)$ at $T/T_c = 0, 0.8, 0.88$ (solid lines from top to bottom), and 1.0 (dashed line); (b) $\chi''(\mathbf{q}, \omega)$ at $T/T_c = 0, 0.8, 0.88$ (solid lines at decreasing incommensurability), and 1.0 (dashed line). The broad and weak commensurate peak in the normal state is seen to grow into sharp and strong commensurate peak at $T = 0.88T_c \lesssim T_c$, and splits into IC peaks that recede from \mathbf{Q}_{AF} at $T \rightarrow 0$. We have truncated the strong commensurate peak for obvious reason. $T_c = 0.25\Delta(0)$, and the T -dependence of $\Delta(T)$ is assumed as the same as in Fig. 3(b). Other parameters are referred to Fig. 9.

rate resonance peak predicted by RPA theories is necessarily softened by temperature. But it will not be continuously softened down to zero, since the onset jump in $\chi''(\mathbf{Q}_{AF}, \omega)$ needs an appreciable nonzero Δ/t . The peak could vanish before its softening is realized and the similar is true for the softening of commensurate peak in $\chi''(\mathbf{Q}_{AF}, \omega)$ [14].

Figure 11 plots the temperature-evolution of the low frequency spectrum in momentum space. The most notable should be the softened commensurate resonance at $\omega \lesssim \omega_o(T = 0)$. When the system is cooled down from above T_c in this frequency regime, the broad and weak commensurate peak in the normal state grows into sharp and strong commensurate peak at some temperature just below T_c , then splits up into IC peaks and recede from \mathbf{Q}_{AF} to a fixed location at low temperature. $1/\chi'_o(\mathbf{q}, \omega)$ also exhibits similar “incommensurate” minimum as in the zero temperature case. Not shown here, the weak

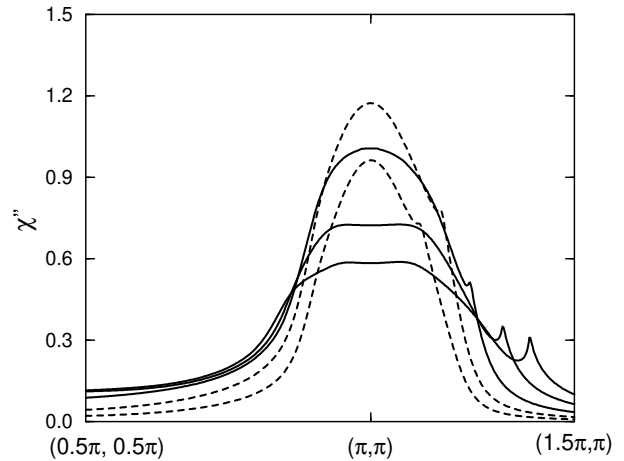


FIG. 12. The broad commensurate peak of normal state $\chi''(\mathbf{q}, \omega)$ at $\omega/\Delta(0) = 0.2, 0.4$ (dashed lines from bottom to top), $0.8, 1.4$, and 2.0 (solid lines from top to bottom). $T = T_c = 0.25\Delta(0)$. Refer those not stated parameters to Fig. 9.

IC structure in SC state at $\omega > \omega_o(T = 0)$ is simply smeared off to a broad commensurate at warming up to the normal state.

Although the above “shoot and split” behavior of the $\omega < \omega_o(T = 0)$ spectrum at the cooling down is already contained in the vHS scenario of $\chi''_o(\mathbf{q}, \omega)$ [14], the normal state commensurate structure always has an intensity higher than the low temperature IC structure in $\chi''_o(\mathbf{q}, \omega)$ [see, for example, a similar case in Fig. 3(b)]. The observed relative excitation intensity in the course of the evolution [see Fig.4 in Ref. [2]] can only be correctly obtained in $\chi''(\mathbf{q}, \omega)$ via an appreciable interaction strength.

A weak and broad commensurate structure is always seen in the normal state at all frequencies [see Fig. 12]. For the dispersion taken here, its intensity reaches a maximum at some $\omega/\Delta(0) \simeq 0.4$ at increasing frequency as a result of the competition between the growing χ''_o and fading RPA-enhancement. Its width is roughly unchanged for $\omega/\Delta(0)$ within $0.8 \sim 1.4$, while grows with frequency at outside the range. A remark is that the similar commensurate structure in χ''_o has intensity and width monotonous increased by frequency. A similar broad peak is also seen in the experiments [2,1].

To make a summary, the exceptional presence of the commensurate peak in YBCO and BSCCO is probably a natural consequence of the approaching of \overline{M} -point vHS to the Fermi level. The diverging incommensurability at $\omega > \omega_o$ in the SC state, and normal state broad commensurate structure at any frequency also find a natural explanation in the scenario. The gross features of the bare and RPA spectra are the same. In a finer comparison, the recent observation on the relative excitation intensity in the normal and SC state slightly prefers the RPA-correction in the resonance regime over the bare

theories. Including the underdoped sample by Arai *et al.* [1] and the nearly optimally doped sample by Bourges *et al.* [2], the back and forth shifting of the IC peaks has a straightforward explanation in the FL picture.

VII. ANISOTROPY EFFECT

Anisotropy effect in the high- T_c cuprates was discussed before by Rendell and Carbotte [4]. The effect is believed to be important in systems such as the orthorhombic crystals or the chained-YBCO. In those systems, anisotropy may either exist in the band dispersion or enter into the SC order parameter, or exist in both. It was pointed out in Ref. [4] that if only one of those two kinds of anisotropy exist in the system, it can be distinguished by the criterion that the gap anisotropy exist only in the SC state while the dispersion anisotropy persists into the normal state. Some important effects of it which can be seen in INS spectrum are, if there is an admixture of s -component in the d -wave gap then there should be a rendering of the four-fold symmetry of the quasielastic node-to-node IC peaks to two-fold, and regardless of the anisotropy source a difference of the nesting IC peak intensities on different crystal axis should be observed.

We will discuss here a case of anisotropy in the gap, the existence of an s -component and the SC order parameter has the form $\Delta_{\mathbf{k}} = \Delta(T)[a s_{\mathbf{k}} + (1-a)d_{\mathbf{k}}]$, where $s_{\mathbf{k}} = 1$ and $d_{\mathbf{k}} = (\cos k_x - \cos k_y)/2$. The existence of an s -component is suggested by the tunneling experiments [32–34] and its percentage is at $a \sim 0.2$. It was discussed in Ref. [4] at low frequencies, but in order to clearly distinguish the effect we think that it is necessary to study its ω -dependence.

Figure 13 shows the contrast of the nesting IC peaks along different crystal axis at different ω , on a system with reasonable size of s -component in the gap. The difference in peak intensities is seen to be most prominent at low ω , and rapidly decreased at increasing frequency. Since the data by Mook *et al.* (on a detwinned orthorhombic $\text{YBa}_2\text{Cu}_3\text{O}_{6.6}$) [3] is at a somewhat low frequency 24 meV $\sim \Delta(0)$, we believe data on a wider ω range is desirable in order to make definite statement on the origin of the one-dimensional nature.

The difference in peak intensities can be easily explained by the picture given in Sec. IV. The twofold symmetric spectrum has the node-to-node excitation closer to one of the two crystal axis, and excitation away from the nodal excitation is suppressed by the coherence factor, therefore the peaks on one of the axis has lower intensity. This can only dominate at frequencies as low as $\sim \Delta$ and excitation along the FS has not been fully opened up.

We have presented here an anisotropy effect suggested by the tunneling experiment and it can introduce one-dimensional feature into the INS spectrum (other possibility is also suggested in Ref. [11]). The frequency de-

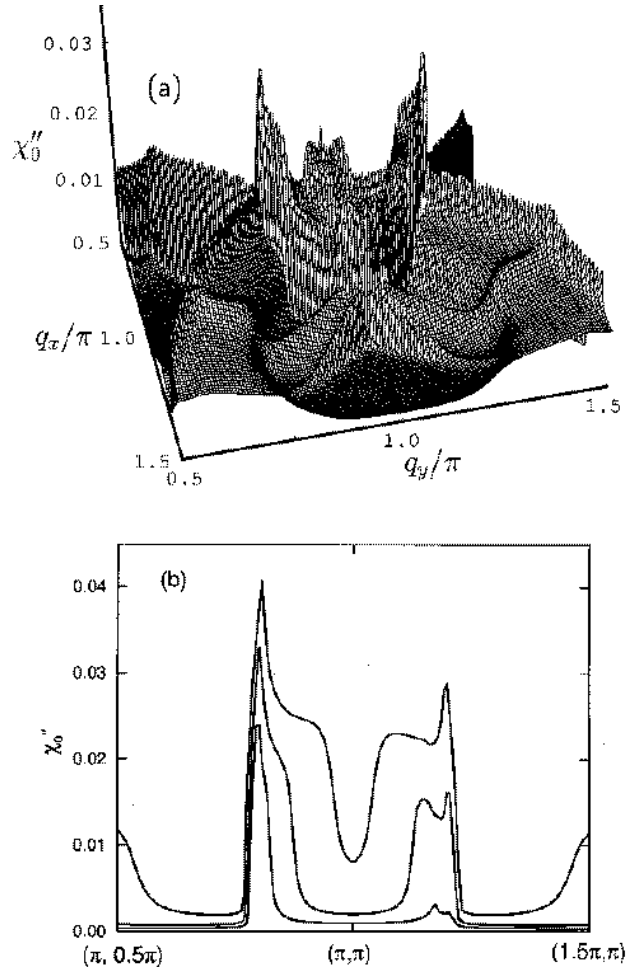


FIG. 13. Anisotropic state $\chi''_o(\mathbf{q}, \omega)$ (a) in the full \mathbf{q} -space at $\omega/\Delta = 1.0$, and (b) along $\mathbf{q} = (\pi, 0.5\pi) - (\pi, \pi) - (1.5\pi, \pi)$ at $\omega/\Delta = 0.6, 0.9$, and 1.2 (from bottom to top). The difference in height of the peaks on different axis is more spectacular at low frequencies. The SC order parameter is taken as $\Delta_{\mathbf{k}} = \Delta[0.2s_{\mathbf{k}} + 0.8d_{\mathbf{k}}]$, where $\Delta = 0.10$, $s_{\mathbf{k}} = 1$, and $d_{\mathbf{k}} = (\cos k_x - \cos k_y)/2$. $T = 0$ and the dispersion is $t = 1$, $t' = -0.25$, and $\mu = -0.65$.

pendence of the contrast of IC peak intensity should act as a criterion to compare with the Stripe interpretation which has no frequency dependence. Furthermore such gap anisotropy effect should vanish in the normal state.

VIII. DISCUSSION AND CONCLUSIONS

We have presented a thorough study on the basic properties of the spin susceptibility and have summarized our findings and comparisons with experiments at the end of each section.

Some possible departure of our conclusions from reality should be mentioned. The presence of impurity in real systems destroys the exact translational symmetry

and mixes states of different momentum, which are also the energy eigenstates. Such process necessarily relaxes the energy conservation selection of the transition region in phase space. The effect should be significant in low energy processes in the SC state where there is inhomogeneous gapping out of phase space by the *d*-wave gap. For example, it may pull down the lower threshold for the existence of the nesting IC peaks [35]. We have also taken a simple *d*-wave in the discussion which is just meant to describe a symmetry with four nodes and change of sign. The actual \mathbf{k} -dependence of the gap should exhibit some deviation from pure *d*-wave since other factors such as interlayer tunneling [36] or correlation effects *etc.* may influence. The important case of possessing a *s*-component was discussed in Sec. VII. The realistic dispersion at the FS also shows deviation from our simple tight-binding band, the most well known of all should be the presence of extended-vHS. Therefore all numerals we give are qualitative.

To a qualitative level, the “inconsistency” between INS spectra of LSCO and YBCO as mentioned in Sec. I can find a consistent picture in the FL interpretation. They could be systems in different regimes of the ratio Δ/v_F . The observations on LSCO [as discussed in Sec. III and Sec. V], including the always IC excitation and incommensurability depends only on doping, necessarily coexist as they are all due to the same limit $\Delta/v_F \ll \pi$. The possibility of RPA commensurate resonance is suppressed in this regime. The observations on YBCO on the other hand [as discussed in Sec. III and Sec. VI], including ω - and T -driven shifting IC peaks in SC state, and normal state broad commensurate peak, necessarily coexist since they are due to deviation from the limit $\Delta/v_F \ll \pi$. The SC state commensurate resonance are ascribed to the approaching of the \bar{M} -point vHS to the Fermi level. That singularity is also an essential piece to explain the diverging incommensurability at $\omega > \omega_o$ in SC state. A peculiar but straightforward conclusion is, the commensurate resonance can occur at $\omega \lesssim \omega_o(T=0)$ when $T \lesssim T_c$, either in bare or RPA theories. This naturally explains the observed enhancement of scattering intensity at \mathbf{Q}_{AF} in that regime [see Fig.4(c) in Ref. [2]].

We would like to point out that while the observed commensurate peak in the SC state could easily find an interpretation as a resonance, as it occurs at a small frequency window; the lower intensity broad commensurate peak in the normal state which is observed at *any* frequency is hard to be interpreted in terms of a resonance. In our scenario this is a natural consequence of the overlap of broad IC peaks, further enhancement by the \bar{M} -point vHS and possibly also by the RPA-correction.

On the ratio Δ/v_F of LSCO and YBCO, there should be a consensus that the SC gap of LSCO (~ 10 meV) is a fraction of that of YBCO (~ 30 meV). Due to the resolution in the determination of the electronic dispersion (say, the resolution in ARPES measurements is about $10 - 40$ meV) and technical problems involved in sample preparation, at present v_F could not be precisely determined

in every material and neither the ratio Δ/v_F [37].

There are some bewildering stems from our work. In the underdoped cuprates, anomalies such as the pseudo-gap phenomenon or the destruction of FS [38] are seen near the maximum gap region and it is likely that the FL picture is to breakdown at that region. But now the FL behavior near the maximum gap region is an important ingredient in our scenario on the YBCO, and our coverage includes both the underdoped and optimally doped YBCO. It seems that to some extent the FL behavior is still retained in the response to INS measurements.

In conclusion, albeit the FL picture on the cuprates is recently quested by many experiments, most behaviors of the recent INS data are still well described in terms of the Fermi liquid picture in its simplest form.

ACKNOWLEDGMENTS

KKV acknowledges the scholarship from NSC of Taiwan under grant No.89-2112-M-003-009. We thank P. Bourges *et al.* for sending us their results prior to publication. We also want to thank A. Abrikosov for sending us his preprint as well as useful correspondences.

- [1] M. Arai, T. Nishijima, Y. Endoh, T. Egami, S. Tajima, K. Tomimoto, Y. Shiohara, M. Takahashi, A. Garrett, and S.M. Bennington, Phys. Rev. Lett. **83**, 608 (1999).
- [2] P. Bourges, Y. Sidis, H.F. Fong, L.P. Regnault, J. Bossy, A. Ivanov, and B. Keimer, Science **288**, 1234 (2000).
- [3] H.A. Mook, P. Dai, F. Dogan, and R.D. Hunt, Nature **404**, 729 (2000).
- [4] J. Rendell and J. Carbotte, Phys. Rev. B **53**, 5889 (1996).
- [5] B. Lake, G. Aeppli, T.E. Mason, A. Schroeder, D.F. Morrow, K. Lefmann, M. Isshiki, M. Nohara, H. Takagi, and S.M. Hayden, Nature **400**, 43 (1999).
- [6] K. Yamada, C.H. Lee, K. Kurahashi, J. Wada, S. Wakimoto, S. Ueki, H. Kimura, Y. Endoh, S. Hosoya, G. Shirane, R.J. Birgeneau, M. Greven, M.A. Kastner, and Y.J. Kim, Phys. Rev. B **57**, 6165 (1998).
- [7] J.M. Tranquada, J.D. Axe, N. Ichikawa, A.R. Moodenbaugh, Y. Nakamura, and S. Uchida, Phys. Rev. Lett. **78**, 338 (1997).
- [8] P. Dai, H.A. Mook, and F. Dogan, Phys. Rev. Lett. **80**, 1738 (1998).
- [9] H.F. Fong, P. Bourges, Y. Sidis, L.P. Regnault, A. Ivanov, G.D. Gu, N. Koshizuka, and B. Keimer, Nature **398**, 588 (1999).
- [10] H.A. Mook, F. Dogan, and B.C. Chakoumakos, cond-mat/9811100.
- [11] P. Bourges, B. Keimer, L.P. Regnault, and Y. Sidis, cond-mat/0006085.
- [12] Y.-J. Kao, Q. Si, and K. Levin, Phys. Rev. B. **61**, R11898 (2000).

[13] M. Norman, Phys. Rev. B **61**, 14751 (2000).

[14] K.-K. Voo and W.C. Wu, cond-mat/9911321.

[15] F. Onufrieva and P. Pfeuty, cond-mat/9903097.

[16] J. Brinckmann and P. Lee, Phys. Rev. Lett. **82**, 2915 (1999).

[17] V. Emery and S. Kivelson, Physica C **235-240**, 189 (1994).

[18] J.M. Tranquada, B.J. Sternlieb, J.D. Axe, Y. Nakamura, S. Uchida, Nature **375**, 561 (1995).

[19] H. Mook and F. Dogan, Nature **401**, 145 (1999).

[20] J. Ma, C. Quitmann, R.J. Kelly, P. Almeras, H. Berger, G. Margaritondo, and M. Onellion, Phys. Rev. B **51**, 3832 (1995).

[21] K. Gofron, J.C. Campuzano, A.A. Abrikosov, M. Lindroos, A. Bansil, H. Ding, D. Koelling, and B. Dabrowski, Phys. Rev. Lett. **73**, 3302 (1994).

[22] D.M. King, Z.-X. Shen, D.S. Dessau, D.S. Marshall, C.H. Park, W.E. Spicer, J.L. Peng, Z.Y. Li, and R.L. Greene, Phys. Rev. Lett. **73**, 3298 (1994).

[23] D.S. Dessau, Z.X. Shen, D.M. King, D.S. Marshall, L.W. Lombardo, P.H. Dickinson, A.G. Loeser, J. DiCarlo, C.-H. Park, A. Kapitulnik, and W.E. Spicer, Phys. Rev. Lett. **71**, 2781 (1993).

[24] K. Gofron, J.C. Campuzano, H. Ding, C. Gu, R. Liu, B. Dabrowski, B.W. Veal, W. Cramer, and G. Jennings, J. Phys. Chem. Solids **54**, 1193 (1993).

[25] J.P. Lu, Phys. Rev. Lett. **68**, 125 (1992).

[26] A.A. Abrikosov, preprint.

[27] A.A. Abrikosov, Phys. Rev. B **57**, 8656 (1998).

[28] V.M. Krasnov, A. Yurgens, D. Winkler, P. Delsing, and T. Claeson, Phys. Rev. Lett. **84**, 5860 (2000).

[29] T. Sato, T. Yokoya, Y. Naitoh, T. Takahashi, K. Yamada, and Y. Endoh, Phys. Rev. Lett. **83**, 2254 (1999).

[30] K. Gorny, O.M. Vyaselev, J.A. Martindale, V.A. Nandor, C.H. Pennington, P.C. Hammel, W.L. Hults, J.L. Smith, P.L. Kuhns, A.P. Reyes, and W.G. Moulton, Phys. Rev. Lett. **82**, 177 (1999).

[31] P.V. Bogdanov, A. Lanzara, X.J. Zhou, S.A. Kellar, D.L. Feng, E.D. Lu, J.-I. Shimoyama, K. Kishio, Z. Hussain, and Z.-X. Shen, cond-mat/0005394.

[32] K.A. Kouznetsov, A.G. Sun, B. Chen, A.S. Katz, S.R. Bahcall, J. Clarke, R.C. Dynes, D.A. Gajewski, S.H. Han, M.B. Maple, J. Giapintzakis, J.-T. Kim, and D.M. Ginsberg, Phys. Rev. Lett. **79**, 3050 (1997).

[33] R. Kleiner, A.S. Katz, A.G. Sun, R. Summer, D.A. Gajewski, S.H. Han, S.I. Woods, E. Dantsker, B. Chen, K. Char, M.B. Maple, R.C. Dynes, and J. Clarke, Phys. Rev. Lett. **76**, 2161 (1996).

[34] A.G. Sun, D.A. Gajewski, M.B. Maple, and R.C. Dynes, Phys. Rev. Lett. **72**, 2267 (1994).

[35] S. Quinlan and D. Scalapino, Phys. Rev. B **51**, 497 (1995).

[36] L. Yin, S. Chakravarty, and P. W. Anderson, Phys. Rev. Lett. **78**, 3559 (1997).

[37] Very recently there is a report of a comprehensive ARPES measurement on LSCO by A. Ino *et al.* in cond-mat/0005370. As debates on ARPES measurements frequently occur, such as the FS is hole- or electron-like in BSCCO [see P.V. Bogdanov *et al.*, cond-mat/0005394, and references therein], and the existence or not of an extended-vHS in Sr_2RuO_4 [see A.V. Puchkov *et al.*, Phys. Rev. B **58**, R13322 (1998), and references therein], we think that it is still early to discuss the effect of the result by A. Ino *et al.* on our conclusion.

[38] D.S. Marshall, D.S. Dessau, A.G. Loeser, C-H. Park, A.Y. Matsuda, J.N. Eckstein, I. Bozovic, P. Fournier, A. Kapitulnik, W.E. Spicer, and Z.-X. Shen, Phys. Rev. Lett. **76**, 4841 (1996).